Search for Invisible Decay of Orthopositronium

T. Mitsui, R. Fujimoto, Y. Ishisaki, Y. Ueda, Y. Yamazaki, S. Asai, and S. Orito
Department of Physics, Faculty of Science, University of Tokyo, Tokyo 113, Japan
(Received 21 January 1993)

Orthopositronium (*o*-Ps) decay or conversion into "invisible" final states is searched for by measuring the energy deposited in a hermetic photon detector for each positron produced from β^+ decay of ^{22}Na and stopped by an aerogel target. No invisible event is detected for a total of 10^8 stopping positrons, thereby giving an upper limit of 2.8×10^{-6} on the *o*-Ps branching ratio, which is 200 times more stringent than previous limits. This experiment excludes an invisible decay as the origin of the reported discrepancy on *o*-Ps lifetime, provides a limit of $\epsilon < 1.5\times10^{-8}$ on the photon-mirror-photon mixing, and rules out millicharged particles lighter than 500 keV.

PACS numbers: 36.10.Dr, 12.20.Fv

The decay rate of orthopositronium (*o*-Ps) in vacuum has been repeatedly measured [1] and is found to be higher than the QED predictions [2] by 1400 ppm, corresponding to 6.3 standard deviations. In attempts to explain the origin of this discrepancy, various exotic decay modes of *o*-Ps have been searched for without obtaining any evidence so far: The decay into a photon and a long-lived, weakly interacting particle (γX^0) was ruled out at a 1-ppm sensitivity level for a mass less than 800 keV [3], while that into a photon and a short-lived particle with a mass greater than 200 keV was also ruled out at 200 ppm [4]. The decay into two photons is also excluded at 350 ppm [5].

As another possible origin of the decay rate discrepancy, Glashow hypothesized [6] *o*-Ps conversion into an "invisible" final state of mirror *o*-Ps via photon-mirror-photon mixing *à la* Holdom [7], and obtained a constraint on the mixing strength from the theory of big bang nucleosynthesis [8]. It has also been postulated that the invisible final state may occur due to *o*-Ps decay into particles of small noninteger electric charge (millicharged particles) [9], which would pass through detectors with little ionization. Existence of such particles is speculated using models which contain an extra U(1) gauge group associated with a mirror universe sector [10]. Although there exist various constraints for millicharged particles [9], those with an electric charge around $10^{-3}e$ (e is the electric charge of an electron) are still allowed, which could explain the decay rate discrepancy of *o*-Ps.

We report in this Letter on a highly sensitive search for *o*-Ps decay or conversion into invisible final states. Although Atoyan *et al.* [11] performed a similar experiment that obtained an upper limit on the branching ratio of 580 ppm, their method necessitated applying a large background subtraction (20000 minus 20000 ppm), where a small change in background between the real and dummy targets could result in error. In contrast, here a thick hermetic photon detector is used to completely eliminate the background of the two escaping photons, hence enabling us to reach a sensitivity 200 times better than Atoyan *et al.* We should then be able to conclude, without any ambiguity, whether the invisible decay or the conversion is the origin of the decay rate discrepancy. Even in the case of a null candidate event, the resultant limit on the invisible branching ratio can be utilized to place a stringent limit on photon-mirror-photon mixing and also to exclude the existence of millicharged particles lighter than electrons.

Figure 1 shows a schematic of the experimental setup in which a 0.1-μCi ^{22}Na positron source is deposited on the front side of a 100-μm-thick plastic scintillator (NE104) with a 12-mm diameter. Most positrons emitted toward the scintillator pass through it producing light pulses that are directed to the photomultiplier (PMT) by the thin parabolic mirror. The positrons are stopped in a target of silica aerogel (diameter, 12 mm; thickness, 3 mm; density, 0.1 g cm^{-3}; and typical grain size, 50 Å) and either form positronium, i.e., *o*-Ps and parapositroni-

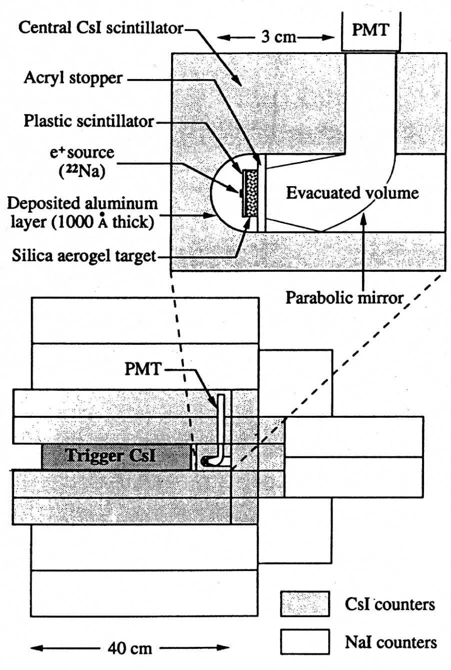

FIG. 1. Schematic of the experimental setup.

um (p-Ps), or annihilate into two photons. A 2-mm-thick acryl stopper is placed behind the target to stop escaping positrons. The silica aerogel target is located in an evacuated volume to reduce the pickoff probability of o-Ps occurring when o-Ps collides with an atomic electron of the target material or of the residual gas, causing annihilation into two photons. The evacuated volume was fabricated by drilling holes into the "central CsI scintillator" which is a part of the hermetic photon detector. The evacuated volume is optically isolated from the central CsI scintillator with a very thin (1000 Å) aluminum layer deposited on the CsI surface to ensure a minimum probability of total photon absorption in front of the CsI counter (2×10^{-9} for the two-photon and less than 10^{-10} for the three-photon states). Even in these extremely rare cases of total photon absorption, the recoil electron has a high probability to penetrate through the materials and deposit enough energy at the CsI scintillator. The ^{22}Na positron source also simultaneously emits a 1275-keV photon that is detected by another CsI scintillator, termed here as the "trigger CsI." This photon signal and the plastic scintillator pulse are used to tag the β^+ decay of ^{22}Na. The central and trigger CsI's are surrounded by 22 CsI counters (weighing 136 kG) and 78 NaI counters (weighing 706 kg). These counters, together with the central CsI scintillator, form a thick hermetic photon detector which detects and measures the total energy of photons produced from the positronium decays or positron annihilations.

Data acquisition is initiated by a coincidence within ±100 ns of the pulses from the plastic scintillator and the 1275-keV photon signal from the trigger CsI. The time interval of the two pulses is recorded by a time-to-digital converter (TDC). The two pulses are also fed to analog-to-digital converters (ADCs) to record the energy information. The pulses from the other CsI and NaI counters are also fed to ADCs. The gates of the ADCs are set to start 100 ns prior to receiving the photon signals from the prompt annihilations and extend 7 μs to make the probability of late o-Ps decay completely negligible.

The energy calibration of the photon counters is performed using the γ-ray peaks from ^{109}Cd, ^{60}Co, and ^{22}Na sources. The counters' energy gain as well as the pedestal of the ADCs are respectively monitored by the 511-keV peak from ^{22}Na and the zero-energy peak. Both peaks are stable to ±0.5 keV throughout the total data acquisition period of 8.7×10^6 s. A total of 9.5×10^7 recorded events can undergo off-line analysis. An obvious background source is the electron capture (EC) decay of ^{22}Na, in which a single 1275-keV photon is emitted without an accompanying positron or other photons. If such an EC photon is accidentally coincident with a fake positron signal such as PMT noise, the event would appear as an invisible decay. To reduce such background, the absolute time difference between the pulses from the plastic scintillator and the trigger CsI is required to be less than 10 ns as shown in Fig. 2(a). This background is eliminated by the further requirement of at least 140 keV deposited on the plastic scintillator [Fig. 2(b)]. The EC decay of ^{22}Na can be another background source, in which the 1275-keV photon Compton scatters in front of or in the plastic scintillator and the recoil electron deposits energy in the plastic scintillator, where the scattered photon is detected by the trigger CsI. This background is eliminated by a tight cut ($1230\ \text{keV} < E_{1275} < 1350\ \text{keV}$) on the energy spectrum of the trigger CsI [Fig. 2(c)].

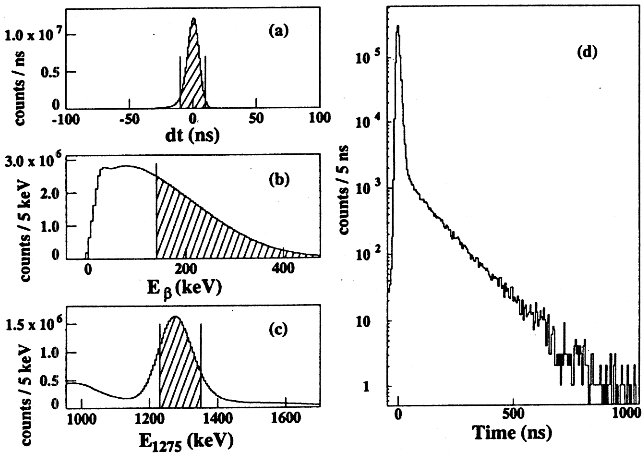

FIG. 2. (a) Time difference pulses from the plastic scintillator and trigger CsI. (b) Positron energy spectrum deposited on the plastic scintillator. (c) γ-ray energy spectrum deposited on the trigger CsI. (d) Time difference between pulses from the plastic scintillator and hermetic photon detector. The prominent peak at $t=0$ is mainly due to prompt annihilations and partially to parapositronium decays, followed by the exponential decay of o-Ps.

For a total of 3.1×10^7 remaining events which is our final data sample of the identified β^+ decay, the energies of all the other counters are summed. Only energy values larger than 2 keV are included to reduce the noise contribution. Figure 3(a) shows the resultant total energy ($E_{\rm tot}$) spectrum. The single prominent peak at $2m_e$ (1022 keV) indicates that a pure sample of positronium decay and positron annihilation is selected. If the positronium decayed or the positron annihilated into invisible states, this would appear as an event with zero deposited energy. As shown in the inset of Fig. 3(a), no such event is detected. According to Monte Carlo simulation, the rate as well as the $E_{\rm tot}$ distribution of the events in the low-energy region are consistent with those expected from the normal two-photon and three-photon final states.

The expected position and shape of the zero-energy peak are determined in a purely experimental manner using the background of EC decay of ^{22}Na. To collect these events, additional data acquisition is performed utilizing only the signal from the trigger CsI as the trigger, i.e., no positron pulse requirement. A total of 1.5×10^6

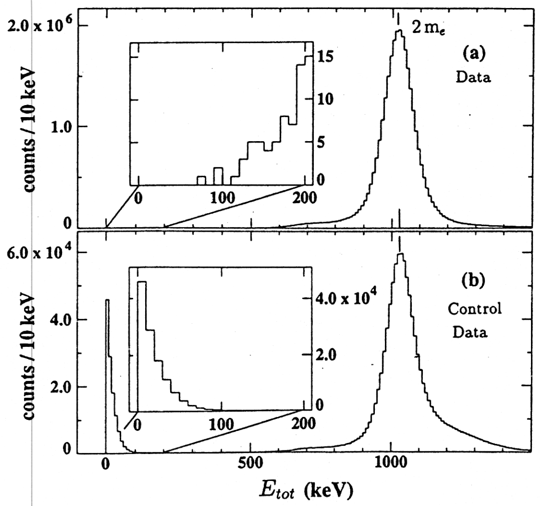

FIG. 3. Total energy spectra deposited on the hermetic photon detector. Insets are the magnified views of the low-energy regions. (a) Data triggered by the coincidence of the pulses from the plastic scintillator and the trigger CsI. (b) Control data sample triggered only with the trigger CsI pulse. The peak at zero energy is due to EC events.

events were obtained for 8.2×10^4 s. Figure 3(b) shows the E_{tot} spectrum of this control data sample after applying the same cut on the energy of the trigger CsI. Note the expected zero-energy peak appears in addition to the 1022-keV peak. The population of the former peak is $(10.32\pm0.03)\%$, being consistent with the EC branching ratio of ^{22}Na (9.5%) after correcting the trigger and selection efficiencies by Monte Carlo simulations. We selected $E_{tot}<50$ keV to define the signal region of the zero-energy event; a region containing 93% of the EC "zero-energy" events below 100 keV. The inefficiency due to accidental background which piles up with the genuine zero-energy event was determined to be 6% by analyzing the randomly triggered events under real data acquisition conditions.

To convert the null result to a limit on the decay branching ratio of *o*-Ps, the formation probability of *o*-Ps is determined as follows. Figure 2(d) shows the time difference distribution between the pulses from the plastic scintillator and hermetic photon detector, taken with the same trigger condition as the actual data acquisition and selected by the same off-line requirements. The sharp peak of the prompt annihilations is followed by the exponential decay curve of *o*-Ps. The formation probability of *o*-Ps is determined from the decay curve to be $(3.3\pm0.1)\%$ per identified β^+ decay of ^{22}Na. Comparing the measured lifetime (134.0 ± 2.5 ns) with the lifetime in vacuum (141.9 ns), the probability of pickoff annihilations is determined to be 5.6%. Correcting for these efficiency factors, the number of $o\text{-Ps}\to3\gamma$ events in the final data sample is determined to be 9.6×10^5. The resultant upper limit is then $B(o\text{-Ps}\to\text{invisible})<2.8\times10^{-6}$ (90% confidence level). This limit is 200 times more stringent than that of Atoyan *et al.* [11], and $\frac{1}{500}$ of the level which would explain the reported discrepancy in the *o*-Ps decay rate. Therefore, the decay or conversion of *o*-Ps into invisible final states is definitely excluded as a major cause of the decay rate discrepancy.

The upper limit on $B(o\text{-Ps}\to\text{invisible})$ can be converted to a limit on the mixing strength between the photon and mirror photon. As shown by Glashow [6], this mixing leads to oscillations between the *o*-Ps and mirror *o*-Ps states. The invisible branching ratio occurring during a long enough observation time can be expressed as

$$B(o\text{-Ps}\to\text{invisible})=\frac{2(2\pi\epsilon f)^2}{\Gamma^2+4(2\pi\epsilon f)^2},$$

where ϵ, Γ, and f are, respectively, the mixing strength between the photon and mirror photon, the decay rate of *o*-Ps into three photons, and the contribution to the ortho-para splitting from the one-photon annihilation diagram involving *o*-Ps. We obtain a direct limit on mixing strength, i.e., $\epsilon<1.5\times10^{-8}$ at 90% confidence level, which is more stringent than the limit (3×10^{-8}) obtained by the theory of nucleosynthesis [8].

The upper limit on $B(o\text{-Ps}\to\text{invisible})$ also constrains the existence of millicharged particles with the electric charge ηe since if they exist, *o*-Ps could decay into a pair of these particles via one-photon exchange. This branching ratio is given by

$$B(o\text{-Ps}\to X\bar{X})=\frac{3\pi\eta^2}{4\alpha(\pi^2-9)}\left[1-\left(\frac{m_X}{m_e}\right)^2\right]^{1/2}\times\left[1-\frac{1}{2}\left(\frac{m_X}{m_e}\right)^2\right],$$

where m_X and m_e are, respectively, the mass of the millicharged particles and electrons and $\alpha=\frac{1}{137}$ is the fine structure constant. The obtained upper limit on the invisible branching ratio then corresponds to the upper limit on the charge ratio $\eta<8.6\times10^{-5}$ for m_X less than 500 keV. The resultant excluded region is shown in Fig. 4, together with existing limits [9].

Our experiment can also be used to obtain the upper limits on the *p*-Ps decay branching ratio and the probability of e^+e^- annihilation into invisible final states. To do this, Monte Carlo simulation was employed to determine the fraction of positrons stopping in the aerogel and in the plastic scintillator and acryl stopper [12], respectively, being 0.13 and 0.87, per identified β^+ decay. By reviewing several previous works [13], we can safely conclude that the minimum and maximum possible formation probabilities of the positronium (*o*-Ps and *p*-Ps included) per stopping positron are 0.4 and 0.6 in the aerogel and 0.2 and 0.4 in the plastic and acryl. In the aerogel, 0.2 to 0.4 of *o*-Ps and 0.05 to 0.1 of *p*-Ps experience the pickoff annihilation in about 2 ns before escaping out of the silica grain. On the other hand, in the plastic and acryl the

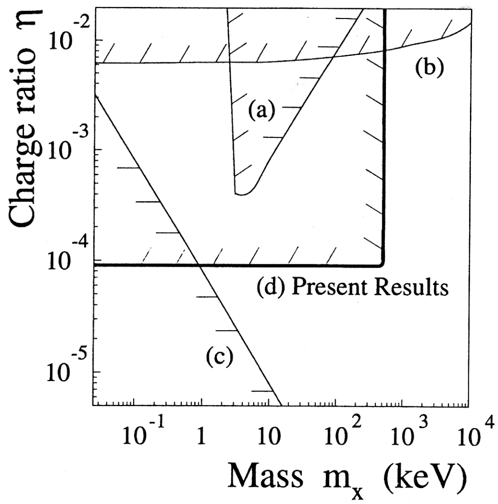

FIG. 4. Constraints for millicharged particles (90% confidence level). (a) Limit from the Lamb shift of a hydrogen atom; (b) limit for the anomalous magnetic moment $(g-2)$ of the electron; (c) astronomical constraint from the cooling time of white dwarfs; (d) region excluded by this experiment.

corresponding pickoff probabilities are 0.99 to 1.0 for *o*-Ps and 0.05 to 0.1 for *p*-Ps. By utilizing proper combinations of these extreme values, one can calculate the smallest possible fractions of *p*-Ps decay and e^+e^- annihilation (including the pickoff) to be 5.1% and 86% per identified β^+, respectively. The resulting upper limits at 90% confidence level are then 1.7×10^{-6} and 1.0×10^{-7} for the *p*-Ps branching ratio and the probability of e^+e^- annihilation, respectively, into invisible final states.

We thank Professor T. Hyodo for his very beneficial discussions, Professor M. Kobayahsi for allowing us to use the NaI counters, and M. Taino for his support.

[1] C. I. Westbrook, D. W. Gidley, R. S. Conti, and A. Rich, Phys. Rev. Lett. **58**, 1328 (1987); Phys. Rev. A **40**, 5489 (1989); J. S. Nico, D. W. Gidley, A. Rich, and P. W. Zitzewitz, Phys. Rev. Lett. **65**, 1344 (1990), and references therein.

[2] W. E. Caswell and G. P. Lepage, Phys. Rev. A **20**, 36 (1979); G. S. Adkins, Ann. Phys. (N.Y.) **146**, 78 (1983); G. S. Adkins, A. A. Salhuddin, and K. E. Schalm, Phys. Rev. A **45**, 3333 (1992); **45**, 7774 (1992).

[3] S. Asai, S. Orito, K. Yoshimura, and T. Haga, Phys. Rev. Lett. **66**, 2440 (1991).

[4] M. Tsuchiaki, S. Orito, T. Yoshida, and M. Minowa, Phys. Lett. B **236**, 81 (1990).

[5] S. Asai, S. Orito, T. Sanuki, M. Yasuda, and T. Yokoi, Phys. Rev. Lett. **66**, 1298 (1991); D. W. Gidley, J. S. Nico, and M. Skalsey, Phys. Rev. Lett. **66**, 1302 (1991).

[6] S. L. Glashow, Phys. Lett. **167B**, 35 (1986); (unpublished).

[7] B. Holdom, Phys. Lett. **166B**, 196 (1986); B **178**, 65 (1986).

[8] E. D. Carlson and S. L. Glashow, Phys. Lett. B **193**, 168 (1987).

[9] M. I. Dobroliubov and A. Y. Ignatiev, Phys. Rev. Lett. **65**, 679 (1990); S. Davidson, B. Campbell, and D. Bailey, Phys. Rev. D **43**, 2314 (1991); R. N. Mohapatra and I. Z. Rothstein, Phys. Lett. B **247**, 593 (1990); R. N. Mohapatra and S. Nussinov, Int. J. Mod. Phys. A **7**, 3817 (1992).

[10] I. Y. Kobzarev, L. B. Okun, and I. Y. Pomeranchuk, Yad. Fiz. **3**, 1154 (1966) [Sov. J. Nucl. Phys. **3**, 837 (1966)]; S. M. Barr, D. Chang, and G. Senjanovic, Phys. Rev. Lett. **67**, 2765 (1991).

[11] G. S. Atoyan, S. N. Gninenko, V. I. Razin, and Y. V. Ryabov, Phys. Lett. B **220**, 317 (1989).

[12] This simulation incorporated the exact geometries of various materials as well as the ionizations and scattering process of the positron. If we take 0.5 as the most likely positronium (*o*-Ps and *p*-Ps included) formation probability in the aerogel, and 0.3 as the pickoff probability in the silica grain, the simulation predicts the fraction of the long-decay *o*-Ps component to be 3.4% per identified β^+, in good agreement with the measured value [$(3.3\pm0.1)\%$].

[13] W. Brandt and R. Paulin, Phys. Rev. Lett. **21**, 193 (1968); F. H. H. Hsu and C. S. Wu, Phys. Rev. Lett. **18**, 889 (1967); P. Kindl and G. Reitar, in *Positron Annihilation*, edited by L. Dorikens-Vanpraet, M. Dorikens, and D. Segers (World Scientific, Singapore, 1989), p. 806; G. Consolati, N. Gambara, and F. Quasso, Z. Phys. D **21**, 259 (1991), and references therein.